Table S1. The comparison of photocatalytic performance with reported 2D g-C_3N_4-based materials and 3D rGO/g-C_3N_4.

Materials	Morphology	photocatalytic performance	Ref.
polystyrene-TiO_2/rGO/g-C_3N_4	2D	RTB dye degradation (51.43%)	[1]
S@g-C3N4 QD sensor	2D	NH_3 response (14.2 kHz)	[2]
X-PCN (X = Cl, Br, or I)	2D	H_2O_2 generation (199.0 μmol h^{-1})	[3]
SCBCN	2D	H_2O_2 generation (620 μmol h^{-1})	[4]
rGO/g-C_3N_4	2D	MO degradation (92.3%)	[5]
g-C_3N_4/rGO	3D	H_2O_2 generation (4.37 mmol g^{-1} h^{-1}) and RhB degradation (96.2%)	This work

Table S2. Specific surface areas and total pore volumes of BCN, PCN, GPCN-1, GPCN-2 and GPCN-3.

Samples	Specific surface areas (m^2 g^{-1})	Total pore volumes (cm^3 g^{-1})
BCN	19.738	0.165
PCN	80.604	0.576
GPCN-1	86.942	0.620
GPCN-2	90.909	0.635
GPCN-3	89.389	0.600

Table S3. The contents of C and N in PCN and GPCN-2 catalysts according to the XPS measurement.

Atomic %	C	N	C/N
PCN	40.96%	57.59%	0.71
GPCN-2	41.98%	57.62%	0.73

Table S4. Lifetime profile and corresponding carrier dynamics information of PCN and GPCN-2.

Samples	**Decay time (ns)**		**Relative amplitude**		**Average lifetime (ns)**
	τ_1	τ_2	A_1	A_2	
PCN	2.43	11.09	128.34	0.42	2.56
GPCN-2	18.87	3.17	0.20	49.33	3.45

Table S5. The comparison of photocatalytic RhB degradation performance with reported g-C_3N_4-based photocatalysts.

Photocatalyst	Light source	irradiation time (min)	RhB degradation rate (%)	Ref.
LSACF/g-C_3N_4	500 W Xe lamp	150	90.1	[6]
BiOI/g-C_3N_4	300 W Xe lamp	75	96	[7]
Fe-g-C_3N_4	300 W Xe lamp	45	95.5	[8]
SAPO-5/g-C_3N_4	500 W Xe lamp	120	94.7	[9]
g-C_3N_4/rGO	500 W metal halide lamp	12	96.2	This work

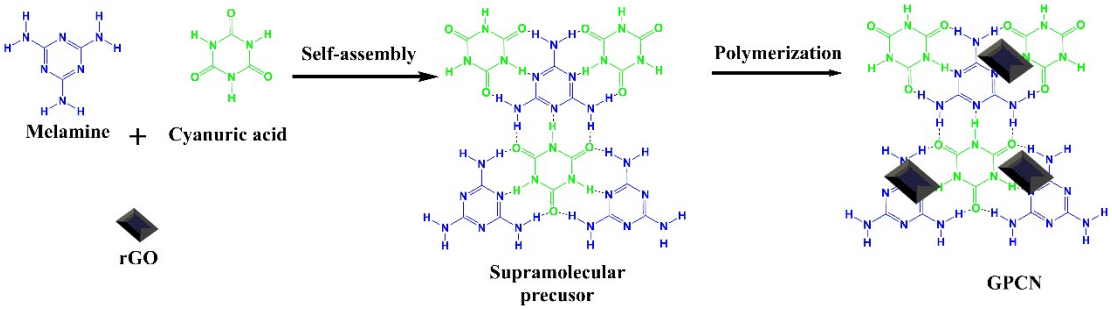

Figure S1. Schematic illustration of the preparation routes for the GPCN.

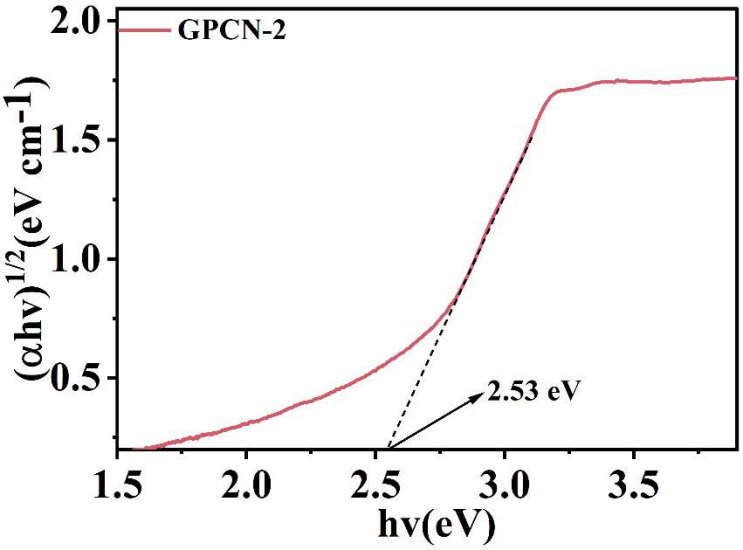

Figure S2. The plots of transformed Kubellka-Munk function versus light energy of GPCN-2.

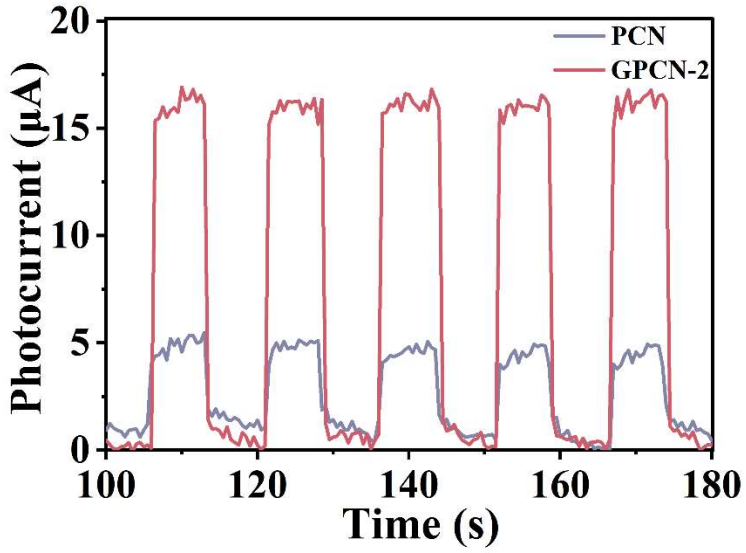

Figure S3. Transient photocurrent of PCN and GPCN-2.

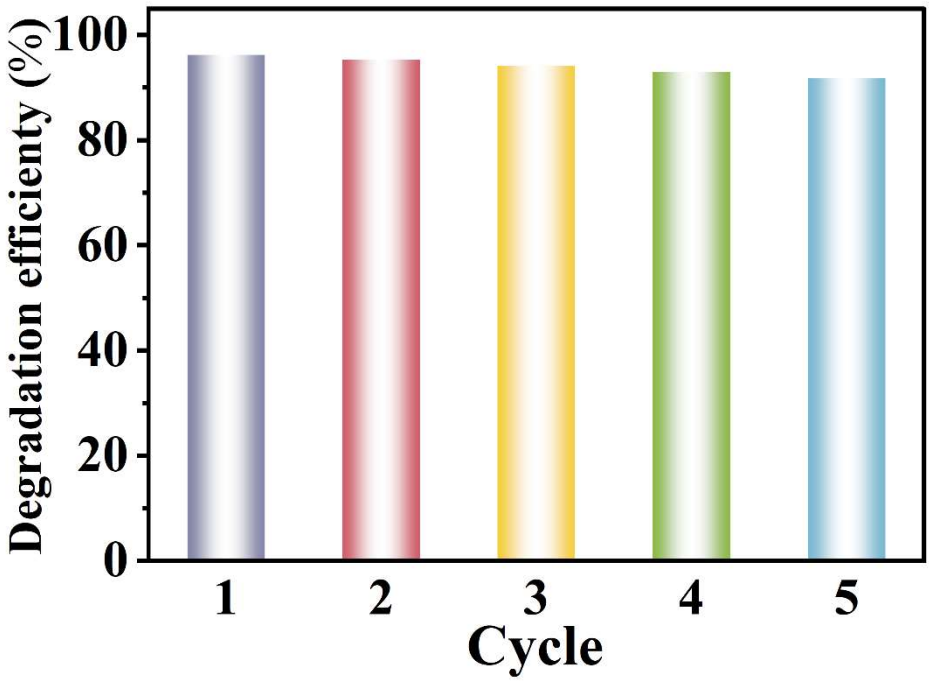

Figure S4. Photocatalytic stability of GPCN-2.

Characterization

X-ray diffraction (XRD) patterns of the catalysts were collected on a Holland Panalytical PRO PW3040/60. The surface chemical status of the samples was characterized by X-ray photoelectron spectroscopy (XPS, Kratos-AXIS ULTRA DLD, Al Kα X-ray source)). The morphologies and structures of the synthesized samples were characterized by field-emission scanning electron microscopy (FESEM, Hitachi S-4800) and high-resolution transmission electron microscopy (HRTEM, JEOL, JEM-2010). UV-Vis diffuse reflectance spectra (DRS) of the prepared samples were obtained by a Hitachi U-3900 spectrophotometer. The room temperature photoluminescence (PL) spectra were examined by fluorescence spectrophotometer (HORIBA Jobin Yvon fluoromax-4) with an excitation wavelength of 385 nm. The Brunauer-Emmett-Teller (BET) specific surface areas of the as-prepared samples were evaluated based on nitrogen adsorption isotherms measured at 77 K using a BELSORP-max nitrogen adsorption apparatus (Micrometitics, Norcross, GA). EIS was performed over a frequency range from 0.1 Hz to 1 MHz at open-circuit potential in 0.1 M Na_2SO_4 solution under Xe light irradiation. Catalyst-loaded indium tin oxides (ITO) electrodes (6 × 6 mm) served as working electrode, a Pt foil as the counter electrode, and an Ag/AgCl electrode as the reference electrode. 10 mg catalyst was uniformly suspended in 1 mL alcohol, then 200 μL suspension was spread on ITO, and EIS could be conducted when the alcohol was completely volatilized.

Photocatalytic H_2 evolution experiments

The photocatalytic H_2 evolution experiments were carried out in glass reaction vessel equipped with a glass closed trace gas analysis system (CEL-PAEM-D8, CEAU Light). Visible light was obtained from a 300 W Xe lamp with a 420 nm cutoff filter (average light intensity: 100 mW cm^{-2}). 50 mg of photocatalysts were added into 100 mL solution (90 mL deionized water and 10 mL triethanolamine as sacrificial agent). 1wt.% Pt as co-catalysts were loaded on the photocatalysts by in situ photo-deposition method using H_2PtCl_6. Before light irradiation, the suspensions were ultrasonically dispersed in the dark for 30 min to achieve absorption-desorption equilibrium. At given time intervals (30 min), a certain amount of produced gas was measured by an online gas chromatograph (GC-2002 N/TFF) equipped with a thermal conductive detector (TCD) and a 5 Å molecular sieve column, using argon as the carrier gas. Product gases were calibrated with standard H_2 gas and their identities were determined according to the retention time.

Photocatalytic degradation experiments

The catalytic performance of catalysts was evaluated by degradation of rhodamine B (RhB). All reactions were carried out in a photochemical reactor (Yanzheng Co., Ltd) with condensed water under stirring. A 500 W of metal halide lamp with 420 nm cutoff filter (average light intensity: 30 mW cm^{-2}) was used as the light source. Briefly, 10 mg of catalyst was ultrasonically dispersed into RhB solution (60 mL, 20 mg L^{-1}), then stirred in darkness for 10 min to achieve an adsorption-desorption balance between catalyst and RhB. During catalytic reaction, 3 mL of suspension was taken out at given time intervals (2 min) and immediately centrifuged to remove the catalyst. The filtrate of RhB was determined with a Hitachi U-3900 UV-vis spectrophotometer and the absorbance value of RhB was used to calculate the concentration at the maximum absorption wavelength.

References

1. Das, S.; Mahalingam, H. Dye degradation studies using immobilized pristine and waste polystyrene-TiO_2/rGO/g-C_3N_4 nanocomposite photocatalytic film in a novel airlift reactor under solar light. *J. Environ. Chem. Eng.* **2019**, *7 (5)*, 103289.
2. Pasupuleti, K.S.; Chougule, S.S.; Vidyasagar, D.; Bak, N.-h.; Jung, N.; Kim, Y.-H.; Lee, J.-H.; Kim, S.-G.; Kim, M.-D. UV light driven high-performance room temperature surface acoustic wave NH_3 gas sensor using sulfur-doped g-C_3N_4 quantum dots. *Nano Res.* **2023**, *16 (5)*, 7682-7695.
3. Gupta, A.; Bhoyar, T.; Abraham, B.M.; Kim, D.J.; Pasupuleti, K.S.; Umare, S.S.; Vidyasagar, D.; Gedanken, A. Potassium molten salt-mediated in situ structural reconstruction of a carbon nitride photocatalyst. *ACS Appl. Mater. Interfaces* **2023**, *15 (15)*, 18898-18906.
4. You, Q.; Zhang, C.; Cao, M.; Wang, B.; Huang, J.; Wang, Y.; Deng, S.; Yu, G. Defects controlling, elements doping, and crystallinity improving triple-strategy modified carbon nitride for efficient photocatalytic diclofenac degradation and H_2O_2 production. *Appl. Catal. B: Environ.* **2023**, *321*, 121941.
5. Li, Y.; Zhang, D.; Chen, Q.; Chao, C.; Sun, J.; Dong, S.; Sun, Y. Synthesis of rGO/g-C_3N_4 for methyl orange degradation in activating peroxydisulfate under simulated solar light irradiation. *J. Alloys Compd.* **2022**, *907*, 164500.
6. Yang, H.; Li, E.; Zhou, B.; Wang, Y.; Li, P.; Xia, S. Preparation and characterization of a g-C_3N_4/LSACF composite and application in RhB degradation. *J Inorg. Organomet. Polym. Mater.* **2020**, *30 (4)*, 1463-1472.

7. Wang, Y.; Zheng, Z.; Li, Y.; Jia, P.; Liu, T. Study on photocatalytic activity of Ag_2O modified BiOI/g-C_3N_4 composite photocatalyst for degradation of RhB. *J. Electron. Mater.* **2022**, *51 (10)*, 5508-5520.

8. Ji, S.; Yang, Y.; Zhou, Z.; Li, X.; Liu, Y. Photocatalysis-Fenton of Fe-doped g-C_3N_4 catalyst and its excellent degradation performance towards RhB. *J. Water Process. Eng.* **2021**, *40*, 101804.

9. Qiu, L.; Zhou, Z.; Ma, M.; Li, P.; Lu, J.; Hou, Y.; Chen, X.; Duo, S. Enhanced visible-light photocatalytic performance of SAPO-5-based g-C_3N_4 composite for Rhodamine B (RhB) degradation. *Materials* **2019**, *12 (23)*, 3948.